

LABORATORY MEASUREMENTS AND ESTIMATES OF THE BIOT COEFFICIENT OF A PRESALT OIL FIELD, SANTOS BASIN

Marcio Jose Morschbacher ¹, Guilherme Fernandes Vasquez  ^{1*},
Julio Cesar Ramos Justen ¹, Marcos Pozzato Figueiredo  ¹,
Flavia de Oliveira Lima Falcão  ², and Ana Lucia Matias Maria  ²

¹Petrobras, Research Center, Cidade Universitária, Ilha do Fundão, Rio de Janeiro, RJ, Brazil

²Petrobras, Centro, Rio de Janeiro, RJ, Brazil

*Corresponding author: vasquez@petrobras.com.br

ABSTRACT. The Biot coefficient is an important parameter in geomechanical models of hydrocarbon reservoirs, with direct influence over the stress distribution in space and time along the production history. We conducted stress-strain experiments (quasi-static measurements) to measure the Biot coefficient of rock samples from an oil field in the Santos Basin. We found strong correlations between these quasi-static measurements and the estimates from dry rock ultrasonic elastic velocities (dynamic measurements). Additionally, we observed good correlations between the Biot coefficients and the effective porosity of the rocks, as well as with the acoustic impedances. These findings suggest that it is possible to derive poroelastic parameter logs of Biot coefficient in well locations, which can be used as input for geostatistical interpolation between wells. This would help in constructing more accurate reservoir geomechanical models and may even enable the generation of a three-dimensional distribution of the coefficient based on acoustic inversion of seismic data.

Keywords: rock physics; geomechanics; poroelasticity.

INTRODUCTION

The Biot coefficient (Biot, 1941; Biot and Willis, 1957) is a crucial parameter for geomechanical models of hydrocarbon reservoir. Its relevance extends also to some geophysical applications, as in seismic production monitoring, for instance.

The Biot coefficient α is defined as:

$$\alpha = 1 - \frac{K_b}{K_m}, \quad (1)$$

where K_b and K_m are the bulk moduli of the drained rock and the solid matrix, respectively.

In Equation (1), K_b gives the resistance of the rock to hydrostatic stress variations, while K_m is the bulk modulus of the solid fraction, including grains and cement materials.

In soil mechanics, the effective stress σ_{ef} is simply the difference between external stress σ and pore pressure P_p , or ($\sigma_{ef} = \sigma - P_p$), because the pore

space of the sediments exhibits very good connectivity. Thus, any increase or decrease in fluid pressure is totally equivalent to an equal increase or decrease in external or confining stress.

However, in consolidated rocks, due to cementation, pore geometries and other factors, not all the variation in pore pressure is transferred to the effective stress. For these rocks, the effective stress is the difference between the external or total stress and the pore pressure weighted by a factor α , the Biot coefficient ($\sigma_{ef} = \sigma - \alpha P_p$).

It is important to note that the elastic moduli of rocks with low Biot coefficient are less sensitive to pore pressure variation. Thus, in a reservoir with low Biot coefficient, the risk of geomechanical issues (fault reactivation, pore collapse etc.) with injection or depletion may be much lower compared to unconsolidated rocks.

Laboratory measurements of the Biot coefficient are not so common because the solid fraction bulk

modulus is difficult to measure due to the low matrix compressibility. Thus, very low strain values are involved in the usual stress-strain relations. For hydrostatic stress variation $\Delta\sigma_{ii}$ causing a volumetric deformation ϵ_v , the corresponding bulk modulus K is given by:

$$K = \frac{\Delta\sigma_{ii}}{\epsilon_v}, \quad (2)$$

These values are generally near the operational limit of sensor (strain gages) sensitivity if we are measuring the matrix deformation (to determine K_m , the matrix modulus).

Rock bulk modulus may be easily and accurately evaluated in experiments with hydrostatic stress variations (with constant pore pressure).

The matrix bulk modulus measurements are possible with hydrostatic stress variations as well, but with unjacketed rock samples, so that the confining and pore pressures are identical and vary exactly the same amount, so that only the solid phase of the rock will deform.

Stress-strain experiments are generally known as static or quasi-static measurements because the frequency of the stress (and strain) variations is very low, even in cyclic stress protocols (frequencies are usually smaller than 0.1 Hz or even 10^{-3} Hz).

If the rocks can be considered elastic and isotropic media, the drained rock bulk modulus can be estimated from elastic-wave velocity measurements in dry rock samples, because the compressional-wave velocity, V_P , and the shear-wave velocity, V_S , depend on the rock bulk and shear moduli, K_b and μ , and the rock density, ρ :

$$V_P = \sqrt{\frac{K_b + \frac{4}{3}}{\rho}}, \quad (3)$$

$$V_S = \sqrt{\frac{\mu}{\rho}}, \quad (4)$$

This kind of estimate is referred as dynamic bulk modulus, because it involves the propagation of relatively high frequency pulses, or oscillations, through the rock (e.g., 800 kHz).

One alternative to evaluate the solid fraction bulk modulus is the use of reference tables, compositional information and some averaging scheme, as the Voigt-Reuss-Hill average, for instance (Mavko et al., 2010).

We present some results of real laboratory measurements of the Biot coefficient for the reservoir rocks of one oil field from the Brazilian Pre-salt, Santos Basin. We compare the experimental results from stress-strain experiments with those derived from velocity propagation measurements and we propose some schemes to derive the Biot coefficient from elastic logs (sonic and density) and compositional information. This procedure may give a detailed and high-resolution Biot coefficient input to

geomechanical models. Alternatively, it is possible to derive the Biot coefficient from reservoir models.

SAMPLE SELECTION

We made this study to check the feasibility of obtaining good Biot coefficient measurements and evaluate if they may be related to other rock properties which are easier and faster to measure, like the dynamic bulk modulus, porosity, or impedance.

We selected eleven rock samples from two wells of the oil field of interest, all from the Barra Velha Formation (which is the main producing reservoir unit of the field) with one exception from the very top of the Itapema Formation.

This selection was strongly based on sample homogeneity, porosity, permeability, and the fact that we observed good waveforms on some of these rock samples in previous dry rock velocity measurements. Moreover, we have good compositional control of these samples based on X-ray diffraction analysis (XRD).

Sample properties and compositional information are listed in Tables 1 and 2. In both tables, the Barra Velha Formation is indicated as “BVE” and the Itapema Formation as “ITP”, the numbers after the acronyms refers to intervals within each zone. The facies are represented as GST for Grainstone, PCK for Packstone, while FLTgst corresponds to a Floatstone with minor Grainstone portion.

MEASUREMENT METHODS

The standard core analysis, including porosity, matrix density and permeability, was made in a gas “permo-porosimeter”, at the estimated in situ effective stress. The porosity measurement uses Helium expansion and Boyle’s law, and permeability measurements use gas flow through the core plug. The porosity uncertainty is around tenths % and, although the permeameter sensitivity is thousandths of mD, for permeable samples, the uncertainty is around tenths of mD. Matrix density uncertainty is around hundredths of g/cm^3 .

We made all the other necessary poroelastic property measurements in a commercial equipment, an AutoLab1000 (made by New England Research Inc.). This system allows measuring one compressional and two shear-wave velocities propagating along the symmetry axis of the cylindrical core plugs, as well as hydrostatic stress-strain measurements with the aid of resistive strain gages. A photograph of the equipment highlighting the main components is shown in Figure 1.

The nominal average frequency of the ultrasonic pulses used for elastic-wave velocity measurements is around 750 kHz. Based on velocity measurements on reference materials and repeated measurements on rock samples, we estimated that the uncertainty of our dynamic results is always below 2%.

Table 1: Facies and petrophysical properties of the studied samples: matrix density ρ_m , effective porosity ϕ , absolute permeability κ and dry bulk density ρ_d . (Facies: GST – grainstone, PCK – packstone, FLTgst – floatstone/grainstone; Formations: BVE – Barra Velha, ITP – Itapema).

Sample			Depth		Petrophysics			
Well	Facies	Zone	Code	MD (m)	ρ_m (g/cm ³)	ϕ (%)	κ (mD)	ρ_d (g/cm ³)
Well #1	GST	BVE200	W1S1	X378.70	2.72	25.2	162	2.03
	GST	BVE310	W1S2	X402.65	2.73	18.4	116	2.23
	GST	BVE320	W1S3	X432.25	2.73	18.5	39	2.22
	GST	BVE320	W1S4	X440.95	2.70	16.8	87	2.25
	GST	BVE320	W1S5	X450.30	2.80	23.3	62	2.15
	GST	BVE320	W1S6	X456.90	2.70	15.8	385	2.27
	GST	BVE330	W1S7	X511.30	2.74	23.1	54	2.11
	PCK	BVE330	W1S8	X519.30	2.70	27.6	202	1.95
Well #2	GST	BVE	W2S1	Y536.90	2.71	17.4	150	2.24
	FLTgst	BVE	W2S2	Y564.08	2.72	19.3	312	2.20
	PCK	Top ITP	W2S3	Y569.13	2.70	19.2	81.6	2.18

Table 2: Composition of the samples used in this case study. (Facies: GST – grainstone, PCK – packstone, FLTgst – floatstone/grainstone; Formations: BVE – Barra Velha, ITP – Itapema).

Sample				Depth					XRD Mineralogy			
Well	Facies	Zone	Code	MD	Calcite	Dolomite	Quartz	Others				
				(m)	(%)	(%)	(%)	(%)				
Well #1	GST	BVE200	W1S1	X378.70	48	43	9	–				
	GST	BVE310	W1S2	X402.65	57	41	2	–				
	GST	BVE320	W1S3	X432.25	66	26	7	1				
	GST	BVE320	W1S4	X440.95	88	7	5	–				
	GST	BVE320	W1S5	X450.30	4	88	8	–				
	GST	BVE320	W1S6	X456.90	85	4	11	–				
	GST	BVE330	W1S7	X511.30	68	28	4	–				
	PCK	BVE330	W1S8	X519.30	100	–	–	–				
Well #2	GST	BVE	W2S1	Y536.90	77	16	6	1				
	FLTgst	BVE	W2S2	Y564.08	86	13	–	1				
	PCK	Top ITP	W2S3	Y569.13	99	–	–	1				

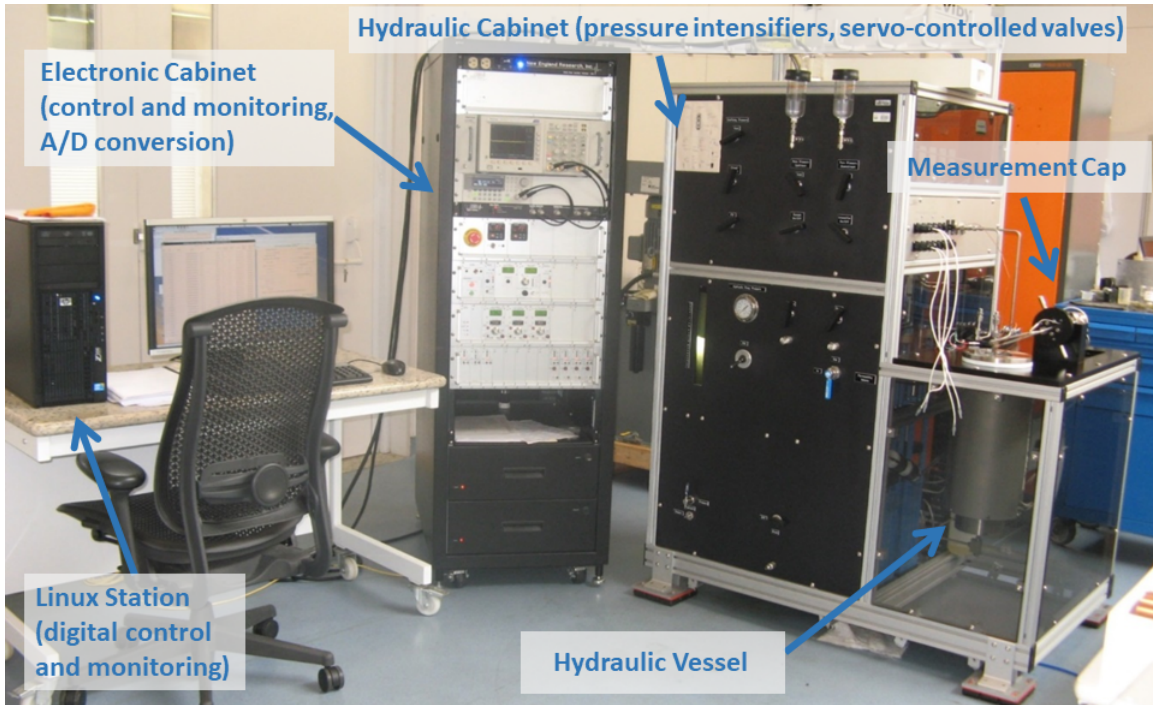


Figure 1: General view of the measurement equipment AutoLab1000.

The samples were jacketed with a copper foil to isolate the pore space from the confining fluid. We attached two horizontal and two vertical strain gages in each sample. The strain gages are linear resistors whose resistance varies as they are deformed, and they are connected to Wheatstone bridges to precisely monitor this resistance variations. Figure 2 shows a photograph of one instrumented sample. First, we measured the dry rock velocities and the dry rock bulk modulus with quasi-static oscillations of the confining stress according to a jigsaw function. We measured the velocities and dry rock bulk modulus from 1000 to 6500 PSI (6.89 to 44.82 MPa) with 500 PSI (3.45 MPa) steps.

After the dry rock experiments on each sample, we saturated the sample with the confining OMA (Óleo Mineral Agrícola) oil and measured the velocities and drained rock bulk modulus with the pore pressure fixed at 0.5 MPa. To measure the matrix bulk modulus, we opened the pore pressure to the confining pressure vessel, detaching the pore pressure tubes. Thus, the pore pressure and confining pressure were totally communicated. Note that the oil will not influence the stress-strain measurements but will modify the velocity measurement results.

We experimented with several stress variation amplitudes, as well as different stress rates. Most experiments were done with a 3.4 MPa amplitude when measuring K_b and 5 to 7 MPa when measuring K_m . Typical stress rates were 0.12 MPa/s and 0.06 MPa/s for these cases.

As we had attached two vertical and two horizontal strain gages to the samples, we made some es-

timates of bulk modulus measurement uncertainties based on all possible combination of strain gages, including the “suppression” of vertical and horizontal elements.

We estimated the dry rock (dynamic) bulk modulus K_d from the elastic-wave velocities and dry rock density ρ_d :

$$K_d = \rho_d \left(V_P^2 - \frac{4}{3} V_S^2 \right) \quad (5)$$

To estimate the dynamic Biot coefficient, we calculated the matrix bulk modulus from the XRD composition and reference tables for mineral bulk modulus using the Voigt-Reuss-Hill (VRH) averaging scheme. All samples were composed mainly of calcite, dolomite and quartz. So, we renormalized the composition of each sample considering only these minerals and used the VRH average as:

$$K_m = \sum_i f_i K_i + \left(\sum_i \frac{f_i}{K_i} \right)^{-1} \quad (6)$$

For the matrix bulk modulus K_m , f corresponds to the amount of each mineral and K to its bulk modulus, with i assuming the corresponding values of calcite, dolomite and quartz. The moduli are listed in Table 3.

We estimated an uncertainty for the results based on the different values observed in a compilation of data from the literature, according to (Wang, 2000; Mavko et al., 2010; Schön, 2011). These values are listed in Table 3.

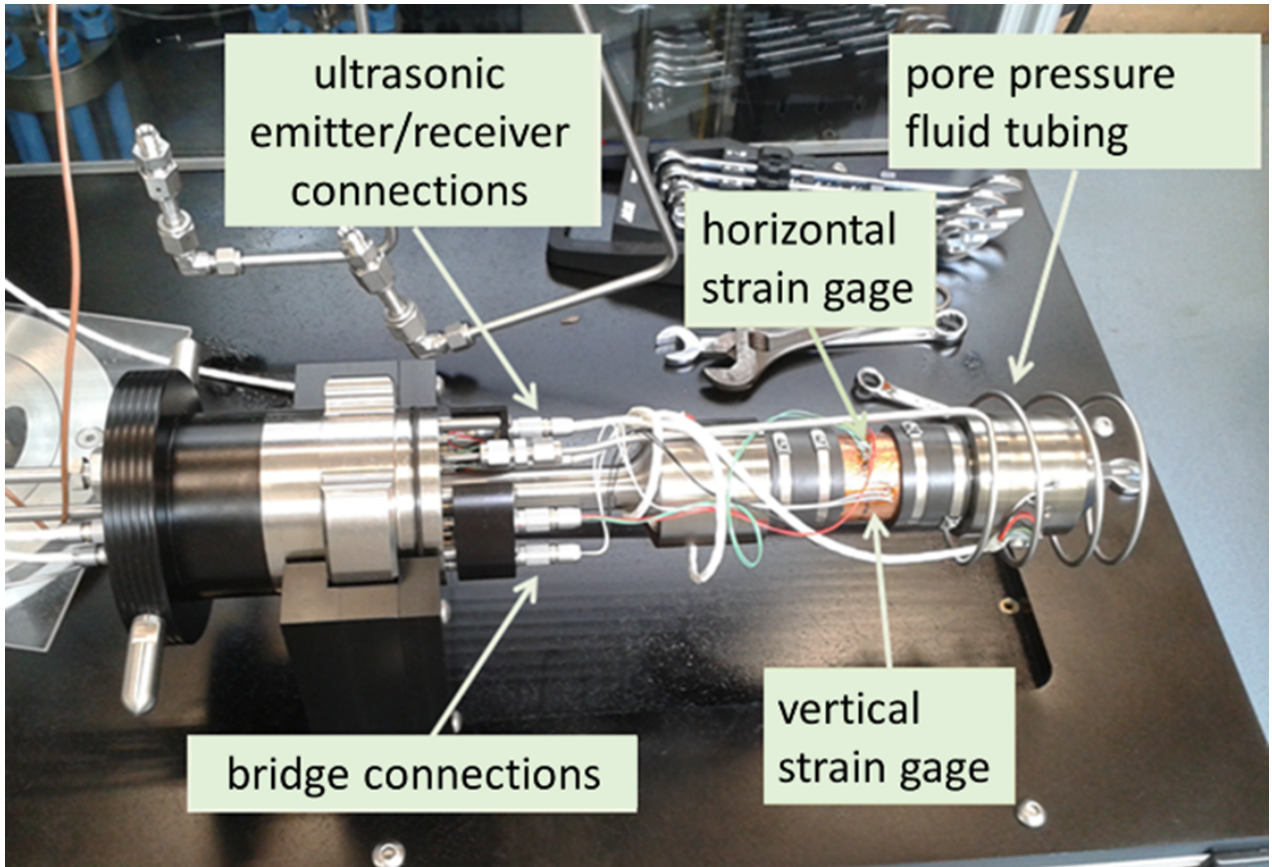


Figure 2: Instrumented sample ready for drained rock bulk modulus and elastic-wave velocity measurements.

We estimated the static or quasi-static Biot coefficient using only the results from stress-strain experiments (rock and solid matrix bulk modulus). There are other experiments that can be used to estimate the Biot coefficient ([Kasani and Selvadurai, 2023](#)).

RESULTS

The results of the direct measurement of the Biot coefficient from quasi-static stress-strain experiments are listed in Table 4, along with the corresponding values estimated from dry rock elastic-wave velocities (dynamic). Although we conducted experiments for various stresses, as described above, the values in this table refer only to the effective stress of 5500 PSI

(37.92 MPa), which is close to the average reservoir conditions.

A comparison between the dynamic and quasi-static bulk modulus of dry rock samples is shown in the scatter plot of Figure 3. The dynamic modulus is usually greater than the static one, as expected ([Fjær et al., 2008](#)). For some samples, the two measurements are virtually equal, within the estimated experimental error. There is one exception: a sample composed mainly of dolomite (W1S5). However, this discrepancy is not so high if we consider the measurement uncertainties. The cause of this discrepancy is not fully understood yet.

Figure 4 illustrates a scatter plot for the drained rock bulk modulus K_d for rock samples from well

Table 3: Mineral bulk modulus with uncertainty estimated from different reference publications, such as Wang (2000), Mavko et al. (2010) and Schön (2011).

Mineral	Bulk Modulus (GPa)	Density (g/cm ³)
Calcite	70 ± 7	2.71
Dolomite	83 ± 12	2.87 ± 0.01
Quartz	37 ± 0.5	2.65
Clay	1.5 to 35	2.13 to 2.75
Silica	25	2.35

Table 4: Biot coefficients for the studied samples from direct measurement (static) and estimated from elastic-wave velocities (dynamic).

Sample		Depth	Biot Coefficient	
Well	Code	MD (m)	α Static	α Dynamic
Well #1	W1S1	X378.70	0.77 ± 0.02	0.76 ± 0.03
	W1S2	X402.65	0.72 ± 0.02	0.68 ± 0.04
	W1S3	X432.25	0.69 ± 0.03	0.64 ± 0.05
	W1S4	X440.95	0.65 ± 0.07	0.59 ± 0.05
	W1S5	X450.30	0.68 ± 0.02	0.70 ± 0.05
	W1S6	X456.90	0.62 ± 0.03	0.56 ± 0.05
	W1S7	X511.30	0.76 ± 0.02	0.70 ± 0.04
	W1S8	X519.30	0.83 ± 0.03	0.76 ± 0.03
Well #2	W2S1	Y536.90	0.60 ± 0.03	0.59 ± 0.05
	W2S2	Y564.08	0.70 ± 0.03	0.66 ± 0.04
	W2S3	Y569.13	0.76 ± 0.03	0.70 ± 0.03

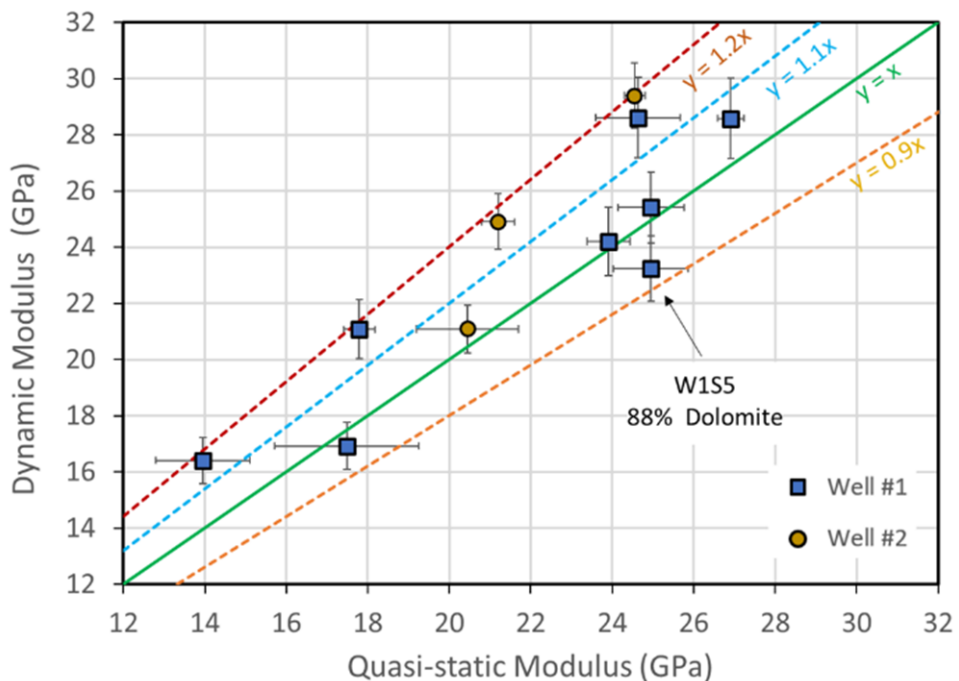


Figure 3: Scatter plot for the results of quasi-static and dynamic drained rock bulk modulus at 5500 PSI (37.92 MPa) confining stress.

#1. There are several points corresponding to the dry rock bulk modulus calculated from legacy velocity measurements (dynamic) and to the new stress-strain bulk modulus measurements (static). The static and dynamic moduli show similar trends, and there is a good correlation between modulus and porosity. A linear fitting to the dynamic data (dashed grey line) gives a correlation coefficient $R^2 = 0.879(K_d = 1.47\Phi + 51.68$, with the porosity Φ in percentage).

We have several legacy velocity measurements in samples with XRD compositional information of rocks from the studied field. As discussed, with velocity data and compositional information, we can estimate the dynamic Biot coefficient.

In Figure 5 we present a scatter plot for the Biot coefficient as a function of sample effective porosity, including static measurements and dynamic estimates. There is an approximate linear relation between Biot coefficient and porosity (although a polynomial function may present a better fitting).

This observation suggests that we can use the porosity from geological model as a proxy to the Biot coefficient. Another alternative would be using the porosity log to derive the coefficient and interpolate between wells using seismic amplitude or seismic inversion as an external drift.

If there are some mineral composition estimates derived from lithogeochemical logs, for instance, we can calculate the dry rock bulk modulus from sonic and porosity logs and fluid information using Gassmann's equation and estimate the matrix modulus from the compositional logs. We observed good agreement between these estimates and our laboratory results as well, as shown in Figure 6. In this case we assumed that the rocks contain only calcite, dolomite and quartz, because other mineral fractions were less or equal to one percent. In this figure the "Biot log" is the continuous dark blue curve, with the associated uncertainty. The values estimated from the velocity data and composition of core plugs are shown in orange diamonds, and the direct Biot coefficients measured are represented by the green squares.

Other interesting correlations are illustrated on Figures 7 and 8. In Figure 7 we show a scatter plot for the Biot coefficient versus core porosity including the laboratory measurement using stress-strain experiments (blue squares and yellow discs) and the coefficient derived from elastic-wave velocities in dry rocks and mineral composition (yellow diamonds and blue triangles, respectively). With the acoustic impedance I_P in these units ($km/s.g/cm^3$), we obtained the relation

$$\alpha = 1.311 - 0.067I_P \quad (7)$$

with coefficient of determination $R^2 = 0.972$. Note that the impedance, in this case, refers to dry rocks, because the drained condition in geophysics (high frequency) is attained only in fluid-free pore space.

In Figure 8 we present a similar version of this graph but including only the Biot coefficient measured by stress-strain experiments. In this plot we included also the ultrasonic saturated rock impedance measured in the laboratory. A good correlation is observed and the corresponding linear regression for saturated rocks is

$$\alpha = 1.402 - 0.067I_P \quad (8)$$

with $R^2 = 0.872$ (continuous green line). Note that the slope of the curve for saturated rocks is equal to the one for dry rocks. In the same graph, the correlation between the Biot coefficient and dry rock acoustic impedance is

$$\alpha = 1.292 - 0.062I_P \quad (9)$$

with $R^2 = 0.866$ (dashed brown line).

DISCUSSION

We measured the "static" and "dynamic" Biot coefficients on a set of carbonate reservoir rocks and observed good correlations between the two data. Note that the "static" Biot coefficient is a real measurement, made with stress-strain experiments to determine the drained rock and the solid matrix bulk moduli. It is relatively expensive to obtain because it demands coring and laboratory measurements. The "dynamic" version of the Biot coefficient is an inference from other measurements. It may involve core measurements, which may be expensive and scarce as well, but it can be derived also from well logs, not so expensive and relatively more abundant. In both cases we derived the rock drained modulus from the elastic-wave velocities and density and estimated the matrix modulus from the composition, reference tables and an averaging scheme.

We observed several correlations between the Biot coefficient and rock properties (e.g, effective porosity and impedance) that would not require assumptions regarding rock composition. Based on these observations we can suggest some methods to estimate Biot coefficient which can be used to build more accurate reservoir geomechanical models:

- Estimate the Biot coefficient from geological model or even from the flow simulation model. This approach may be relatively easy and fast; it would require no interpolation, but probably would not be the best method, especially if we use the large-scale cells from flow simulation model.
- Estimate the Biot coefficient from porosity logs and interpolate between wells with the aid of

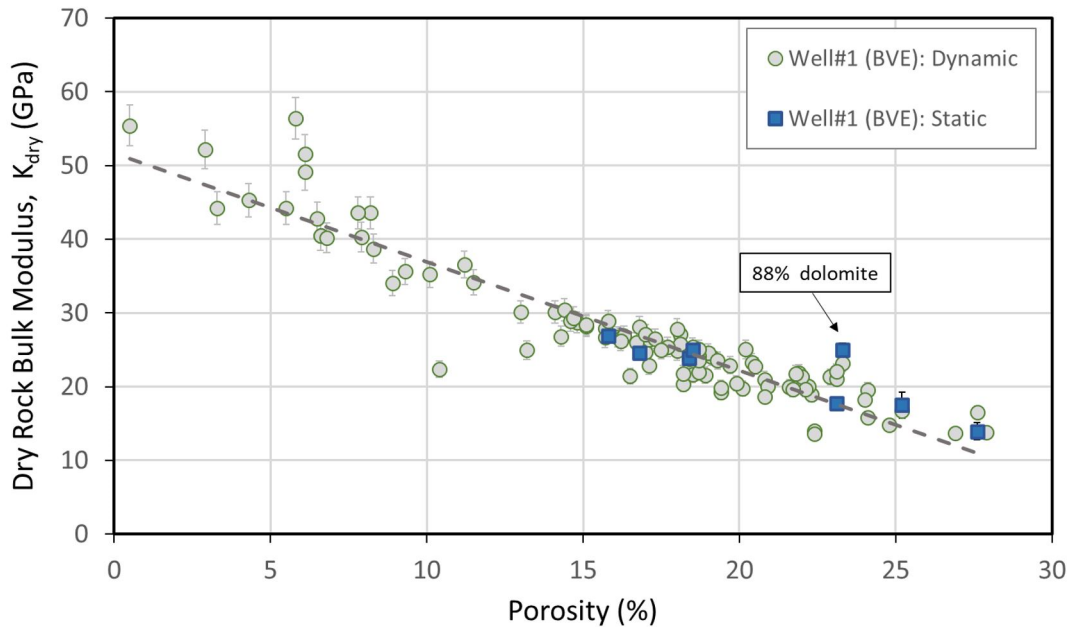


Figure 4: Dry rock bulk modulus as a function of porosity for well #1 samples at 5500 PSI (37.92 MPa).

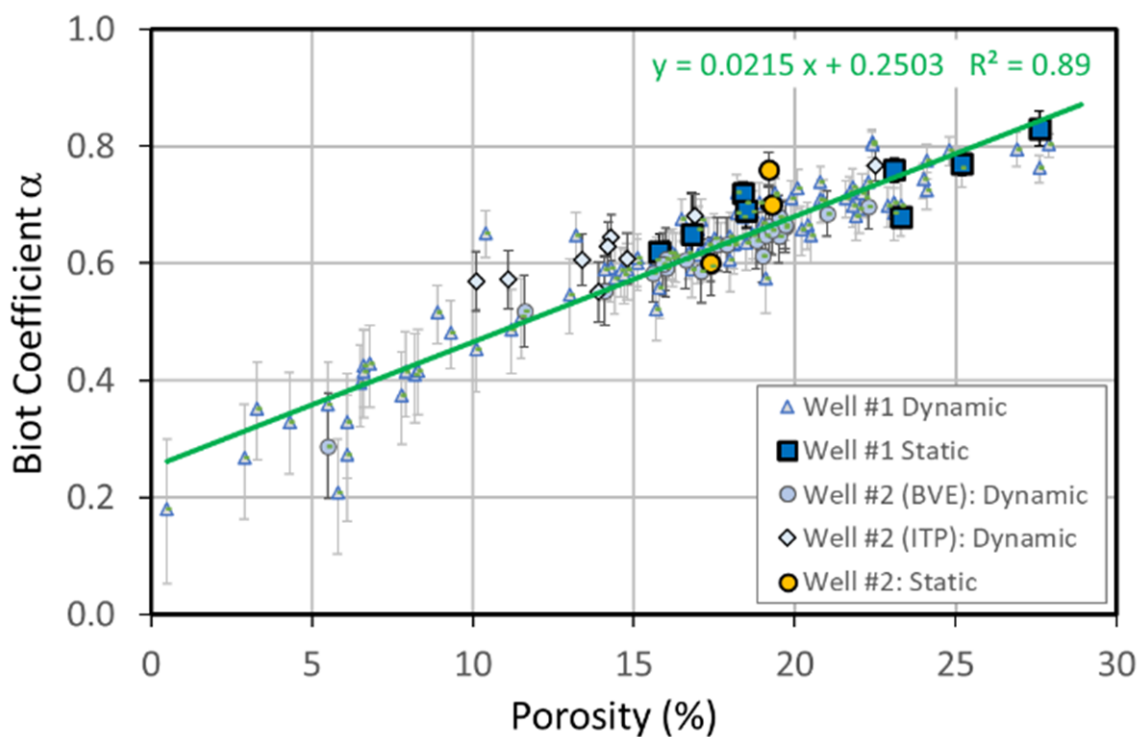


Figure 5: Biot coefficient as a function of porosity for all samples, including legacy data (for the “dynamic” case).

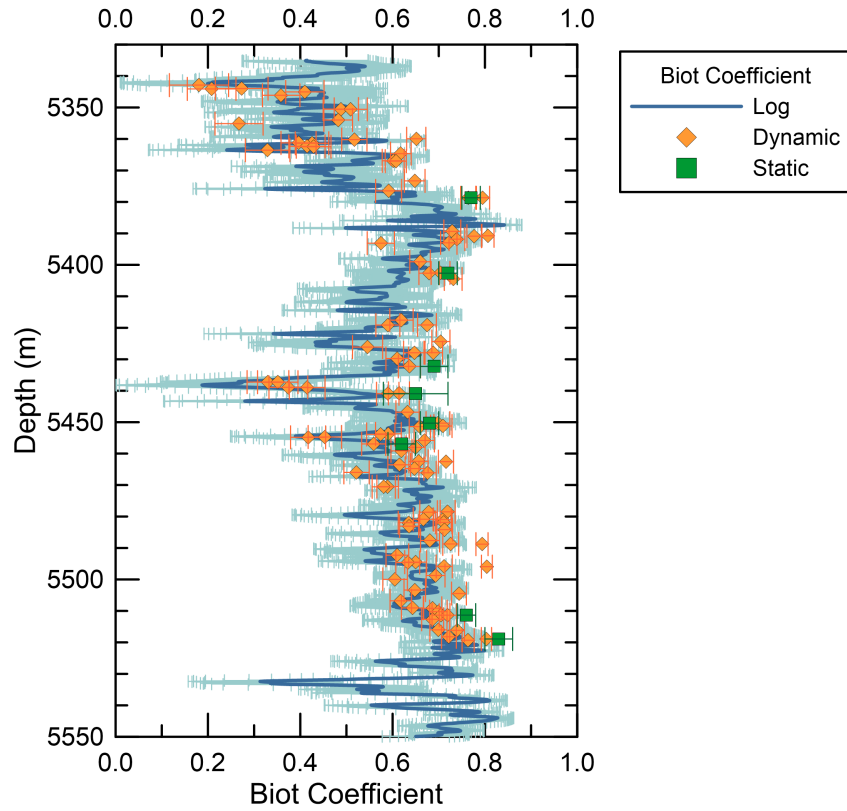


Figure 6: Biot coefficient log for well #1 (continuous line) estimated from acoustic and porosity log and compositional information. The data represented by green squares are the Biot coefficient (static) measured in the laboratory by stress-strain experiments, and the orange diamonds represent the values calculated from laboratory velocity data and composition.

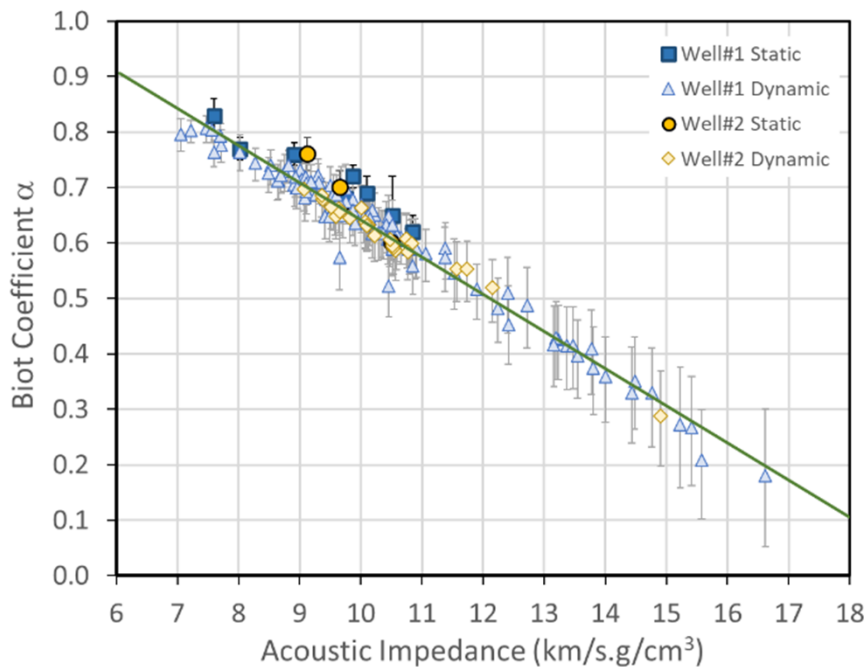


Figure 7: Scatter plot for the quasi-static and dynamic Biot coefficient versus dry rock acoustic impedance.

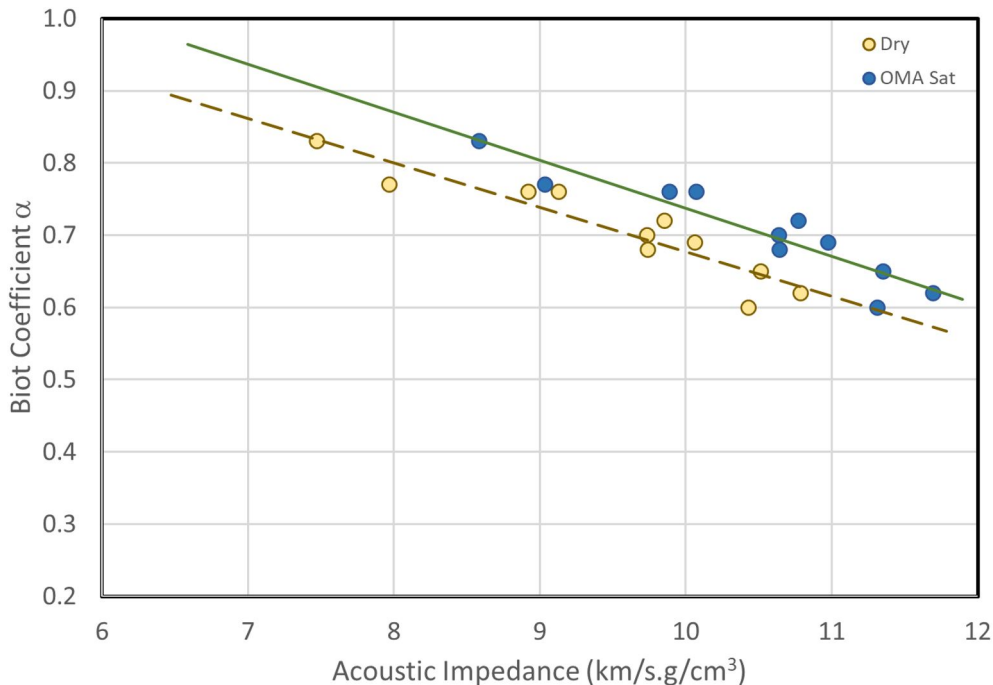


Figure 8: Scatter plot for the quasi-static Biot coefficient versus acoustic impedance for dry and oil saturated rocks.

seismic amplitude or even impedance as an external drift. This approach sounds good, but as we observed that there is a good correlation between Biot coefficient and acoustic impedance, maybe it would be better to use acoustic impedance logs as the starting point.

- Estimate directly from acoustic impedance volumes, because there is a good correlation between the Biot coefficient and acoustic impedance. This would be relatively fast and would require no interpolation, and the details would be related to the seismic resolution.
- Calculate the Biot coefficient at well locations based on the elastic logs, composition and fluid substitution, and then interpolate between wells with the aid of some seismic attribute, maybe the acoustic impedance. This approach requires good control of saturation, fluid properties and compositional logs, and may consume more time compared to other ones.

Most of these comments about the possible approaches to estimate the Biot coefficient are based on intuition and guesses. It would be nice to do some small pilot test to verify the best method.

Indeed, we tested the use of porosity model to estimate the Biot coefficient and obtained good results.

CONCLUSIONS

We measured the Biot coefficient in rock samples from a Pre-salt oil field from the Santos Basin and observed good correlations between these measurements

and the estimates based on dry rock velocity measurements, as well as with the porosity and elastic properties of the rocks.

There is also an excellent agreement between our measurements and the Biot coefficient calculated from well logs.

We suggest some methods to estimate Biot coefficient logs and 3D volumes based on our observations, which can be used to build more accurate reservoir geomechanical models. The choice of the best method demands some practical pilot test.

ACKNOWLEDGMENTS

We thank Petrobras for permission and support to publish this scientific article. Thanks to Ana Paula Martins de Souza and Tiago Manes Nunes for their help. We would like to thank Andre Luis Romanelli Rosa for encouraging the studies and helping to show the importance of geophysicist to geomechanical studies.

REFERENCES

Biot, M. A., 1941, General theory of three-dimensional consolidation: *Journal of Applied Physics*, **12**, 155–164, doi: [10.1063/1.1712886](https://doi.org/10.1063/1.1712886).

Biot, M. A., and D. G. Willis, 1957, The elastic coefficients of the theory of consolidation: *ASME Journal of Applied Mechanics*, **24**, 594–601, doi: [10.1115/1.4011606](https://doi.org/10.1115/1.4011606).

Fjær, E., R. M. Holt, P. Horsrud, A. M. Raaen, and R. Risnes, 2008, *Petroleum related rock mechanics*, 2nd ed.: Elsevier Scientific.

Kasani, H. A., and A. P. S. Selvadurai, 2023, A review of techniques for measuring the biot coefficient and other effective stress parameters for fluid-saturated rocks: *Applied Mechanics Reviews*, **75**, 020801, doi: [10.1115/1.4055888](https://doi.org/10.1115/1.4055888).

Mavko, G., T. Mukerji, and J. Dvorkin, 2010, *The rock physics handbook: Tools for seismic analysis of porous media*, 2nd ed.: Cambridge University Press.

Schön, J., 2011, *Physical properties of rocks. a workbook*, volume **8** of *Handbook of Petroleum Exploration and Production*: Elsevier.

Wang, Z., 2000, The gassmann equation revisited: comparing laboratory data with gassmann's predictions, in *Seismic and Acoustic Velocities in Reservoir Rocks: Recent Developments*: Society of Exploration Geophysicists (SEG), Geophysics Reprint Series, No. 19, 8–23.

Morschbacher, M.J.: sample selection (equal), experimental parameters (equal), result discussions and interpretation (equal), writing – original draft preparation (equal), sample preparation (lead), data acquisition and correlations (lead); **Vasquez, G.F.:** sample selection (equal), experimental parameters (equal), result discussions and interpretation (equal), writing – original draft preparation (equal), sample preparation (equal), data acquisition and correlations; **Justen, J.C.R.:** sample selection (equal), experimental parameters (equal), result discussions and interpretation (equal), writing – original draft preparation (equal), sample preparation (equal), data acquisition and correlations; **Figueiredo, M.P.:** sample selection (equal), experimental parameters (equal), result discussions and interpretation (equal), writing – original draft preparation (equal), sample preparation (equal), data acquisition and correlations; **Falcão, F.O.L.:** sample selection (equal), experimental parameters (equal), result discussions and interpretation (equal), writing – original draft preparation (equal), result application; **Maria, A.L.M.:** sample selection (equal), experimental parameters (equal), result discussions and interpretation (equal), writing – original draft preparation (equal), result application (equal).

Received on November 29, 2023 / Accepted on June 20, 2024



Creative Commons attribution-type CC BY